OXFORD
SOT | Society of Toxicology
www.toxsci.oxfordjournals.org

*TOXICOLOGICAL SCIENCES*, 144(2), 2015, 393–405

doi: 10.1093/toxsci/kfv006
Advance Access Publication Date: January 19, 2015

# *N*-Hydroxylation of 4-Aminobiphenyl by CYP2E1 Produces Oxidative Stress in a Mouse Model of Chemically Induced Liver Cancer

Shuang Wang*, Kim S. Sugamori*, Aveline Tung*, J. Peter McPherson*, and Denis M. Grant*,†,1

*Department of Pharmacology and Toxicology, University of Toronto, Toronto, Ontario, Canada M5S 1A8 and †Leslie Dan Faculty of Pharmacy, University of Toronto, Toronto, Ontario, Canada M5S 3M2

[1]To whom correspondence should be addressed at 1 King's College Circle, Toronto, ON, Canada M5S 1A8. Fax: +1 416-978-6395. E-mail: denis.grant@utoronto.ca.

## ABSTRACT

4-Aminobiphenyl (ABP) is a trace component of cigarette smoke and hair dyes, a suspected human carcinogen and a potent rodent liver carcinogen. Postnatal exposure of mice to ABP results in a higher incidence of liver tumors in males than in females, paralleling the sex difference in human liver cancer incidence. A traditional model of ABP tumorigenesis involves initial CYP1A2-mediated *N*-hydroxylation, which eventually leads to production of mutagenic ABP-DNA adducts that initiate tumor growth. However, several studies have found no correlation between sex or CYP1A2 function and the DNA-damaging, mutagenic, or tumorigenic effects of ABP. Oxidative stress may be an important etiological factor for liver cancer, and it has also been linked to ABP exposure. The goals of this study were to identify novel enzyme(s) that contribute to ABP *N*-oxidation, and to investigate a potential role for oxidative stress in ABP liver tumorigenicity. Isozyme-selective inhibition experiments using liver microsomes from wild-type and genetically modified mice identified CYP2E1 as a major ABP *N*-hydroxylating enzyme. The *N*-hydroxylation of ABP by transiently expressed CYP2E1 produced oxidative stress in cultured mouse hepatoma cells. *In vivo* postnatal exposure of mice to a tumorigenic dose of ABP also produced oxidative stress in male wild-type mice, but not in male *Cyp2e1*(−/−) mice or in female mice. However, a stronger NRF2-associated antioxidant response was observed in females. Our results identify CYP2E1 as a novel ABP-*N*-oxidizing enzyme, and suggest that sex differences in CYP2E1-dependent oxidative stress and antioxidant responses to ABP may contribute to the observed sex difference in tumor incidence.

**Key words**: 4-aminobiphenyl; bioactivation; liver tumorigenesis; oxidative stress; NRF2

Human liver cancer is the third most common cause of death from cancer worldwide, with a 5-year survival rate of only 7% (Bosch *et al.*, 2004; Ferlay *et al.*, 2010). Prevention and treatment of this disease may be achieved with a better understanding of the pathological mechanisms linking particular risk factors, such as chemical carcinogens, alcoholic liver disease, and viral hepatitis, to tumorigenesis. In this regard, rodent liver tumor induction models are valuable tools not only in risk assessment for known and novel chemical entities but also to gain insights into tumorigenic mechanisms as a first step toward the identification of potential novel drug targets.

4-Aminobiphenyl (ABP) is a ubiquitous environmental contaminant of the aromatic amine class of both human and rodent carcinogens (Grimmer *et al.*, 2000; National Toxicology Program, 2014). In humans, ABP exposure has been associated predominantly with an increased incidence of bladder tumors (National Toxicology Program, 2014), and numerous studies have attempted to define mechanisms for this tissue selectivity

(Besaratinia and Tommasi, 2013). In contrast, ABP is commonly used in rodent tumor bioassays as a potent chemical tool to produce tumors selectively in the liver. For instance, exposure of male C57BL/6 mice to only two doses of ABP on postnatal days 8 and 15, according to the standard neonatal tumor bioassay protocol (McClain *et al.*, 2001), leads to the appearance of visible tumors by 1 year of age only in the liver (Kimura *et al.*, 1999; Sugamori *et al.*, 2012).

ABP-induced liver tumor growth in mice also occurs predominantly in males but not in females (Kimura *et al.*, 1999; Sugamori *et al.*, 2012), which parallels the significant sex difference that is observed in the overall incidence of human liver cancer, where men have a 3- to 5-fold higher risk than women even after correcting for exposure to known risk factors (Altekruse *et al.*, 2009; Chen *et al.*, 1997). This sexual dimorphism extends to liver tumors produced by other chemicals such as diethylnitrosamine (Naugler *et al.*, 2007) as well as to tumors arising in a transgenic model of chronic human hepatitis B infection (Kim *et al.*, 1991). Thus, a better understanding of the underlying causes of the sexual dimorphism in mouse models of liver cancer may shed light on the etiology of the human disease, and aid in the identification of novel pathways for its treatment or prevention.

Like other aromatic amines, ABP is thought to require metabolic activation to exert its tumorigenic effects. According to one widely accepted model of ABP bioactivation and resultant liver tumorigenesis in rodents, ABP is first *N*-hydroxylated by the cytochrome P450 isoform CYP1A2 to form *N*-hydroxy-ABP (HOABP), which is subsequently *O*-conjugated by phase II enzymes such as the arylamine *N*-acetyltransferases (NAT1 and/or NAT2) to generate highly unstable ester metabolites (Butler *et al.*, 1989; Orzechowski *et al.*, 1994). The esters spontaneously hydrolyze to highly reactive arylnitrenium ions that form covalent adducts with various cellular macromolecules, including DNA (Chou *et al.*, 1995; Minchin *et al.*, 1992; Novak *et al.*, 1993). In turn, the introduction of ABP-DNA adducts and subsequent mutations into critical tumor promoter and/or suppressor genes initiates the process of liver tumorigenesis (Feng *et al.*, 2002; Parsons *et al.*, 2005).

With the availability of an increasing number of genetically modified mouse strains, selected components of the above model of ABP bioactivation have been tested *in vivo*. In contrast to predictions from the traditional model, *Cyp1a2*(−/−) mice were not protected from ABP-induced C8-dG-ABP adducts, the major form of ABP-DNA adducts, nor from liver tumors (Kimura *et al.*, 1999; Tsuneoka *et al.*, 2003). Similarly, 2,3,7,8-tetrachlorodibenzo[p]dioxin-treated wild-type mice possessing elevated levels of CYP1A2 demonstrated lower, rather than higher, levels of C8-dG-ABP adducts (Tsuneoka *et al.*, 2003). Using the standard neonatal tumor bioassay exposure protocol, we observed that ABP produced no sex differences in the acute level of C8-dG-ABP adducts, mutation frequency, or mutation spectra (Sugamori *et al.*, 2012; Wang *et al.*, 2012). Studies using *Nat1/2*(−/−) mice also showed a lack of correlation between the DNA-damaging and mutagenic properties of ABP and liver tumorigenesis (Sugamori *et al.*, 2012; Wang *et al.*, 2012). Overall, these *in vivo* results support (1) the existence of alternative pathways of ABP bioactivation and/or (2) the existence of as yet uncharacterized factor(s) that drive mouse liver tumorigenesis following ABP exposure, leading to the sex differences that are observed in tumor bioassays.

Aside from forming covalent adducts, ABP has also been shown to produce oxidative stress both *in vitro* and *in vivo* in mouse liver. *In vitro*, ABP produces reactive oxygen species through the redox cycling of the HOABP metabolite (Makena and Chung, 2007; Murata *et al.*, 2001). In one *in vivo* study, a single dose of ABP resulted in the depletion of hepatic thiols more severely in wild-type male mice than in females (Tsuneoka *et al.*, 2003). As oxidative stress represents a major etiological factor for many human liver diseases including liver cancer (Hatting *et al.*, 2009; Hussain *et al.*, 2000), a goal of this study was to investigate the potential role of oxidative stress as a driver of liver tumorigenesis in the ABP neonatal bioassay.

## MATERIALS AND METHODS

*Chemicals and reagents*. HOABP was purchased from Toronto Research Chemicals (Toronto, Ontario, Canada). Minimal essential medium (MEM) (minus phenol red, Cat. No. 51200038), Lipofectamine LTX, TRIzol, random hexamer primers, M-MLV reverse transcriptase, and SYBR Green dye were purchased from Life Technologies Inc (Burlington, Ontario, Canada). Taq DNA polymerase, DNase I, and RiboLock RNase inhibitor were purchased from ThermoFisher Scientific Inc (Burlington, Ontario, Canada). All quantitative PCR (qPCR) primers (Supplementary Table 1) were synthesized by Integrated DNA Technologies Inc (Coralville, Iowa). HPLC grade methanol and acetonitrile were purchased from Caledon Laboratories Ltd (Georgetown, Ontario, Canada). Protease and phosphatase inhibitors were purchased from Roche Diagnostics (Laval, Quebec, Canada). Bio-Rad Protein Assay reagent was purchased from Bio-Rad Laboratories Ltd (Mississauga, Ontario, Canada). Anti-γH2AX antibody was purchased from EMD Millipore Co (Billerica, Massachusetts). Anti-H3 antibody was purchased from Sigma-Aldrich Canada Ltd (Oakville, Ontario, Canada). NRF2 antiserum was kindly provided by Ed Schmidt from the Department of Immunology and Infectious Diseases at Montana State University, Bozeman, Montana. Anti-mouse and anti-rabbit secondary antibodies were purchased from Cell Signaling Technology Inc (Danvers, Massachusetts). Enhanced chemiluminescence (ECL) prime was purchased from GE Healthcare (Baied'Urfe, Quebec, Canada). Hepa1c1c7 cells were purchased from ATCC (Manassas, Virginia). PcDNA3.1(+) expression plasmid containing mouse *Cyp1a2* cDNA was kindly provided by Shigeyuki Uno at the Department of Biomedical Sciences, Nihon University, Itabashi-ku, Tokyo, Japan. PCMV6 expression plasmid containing mouse *Cyp2e1* cDNA was purchased from OriGene Technologies (Rockville, Maryland). Rat CYP2E1 expression plasmids (wild-type and mutants) were kindly provided by Narayan Avadhani from the Department of Animal Biology at the University of Pennsylvania, Philadelphia, Pennsylvania. All other chemicals were purchased from Sigma-Aldrich Canada Ltd.

*Animals and treatments*. All procedures involving animals were performed in accordance with the Canadian Council on Animal Care guidelines and approved by the University of Toronto Animal Care Committee. Breeding stocks of *Cyp1a2*(−/−) mice (on a congenic C57BL/6 genetic background) were kindly provided by Daniel W. Nebert from the Department of Environmental Health, University of Cincinnati Medical Center, Cincinnati, Ohio (Liang *et al.*, 1996). Breeding stocks of *Cyp2e1*(−/−) mice (on a congenic 129S4/SvJae background) were kindly provided by Frank J. Gonzalez at the National Cancer Institute, Bethesda, Maryland (Lee *et al.*, 1996). *Cyp2e1*(−/−) 129S4/SvJae and C57BL/6 mixed-strain mice were generated by crossing *Cyp2e1*(−/−) 129S4/SvJae with C57BL/6 mice, interbreeding the F1 hybrids, and genotyping the F2 offspring for

*Cyp2e1* status. C57BL/6 mice were purchased from Charles River Laboratories Inc (Senneville, Quebec, Canada).

According to the standard neonatal ABP exposure protocol, mice were injected intraperitoneally on postnatal days 8 and 15 with 1/3 and 2/3 of the total dose of ABP, respectively, at a total dose of 1200 nmol (approximately 17 mg/kg per dose), or with the corresponding volumes (10 and 20 μl) of dimethyl sulfoxide (DMSO) vehicle.

*Cell culture and cell transfection*. The Hepa1c1c7 mouse hepatoma cell line was maintained in MEM in the presence of 10% v/v fetal bovine serum, non-essential amino acids, penicillin–streptomycin, and 2 mM L-glutamine. Transient transfection of Hepa1c1c7 cells was carried out using Lipofectamine LTX following the manufacturer's protocol. Briefly, cells were seeded at $5 \times 10^5$ cells per well onto six-well plates, grown overnight, treated with transfection mix (6 μl LTX: 2 μg of DNA for CYP1A2 and 9 μl LTX: 2 μg of DNA for CYP2E1) for 6 h in MEM only, followed by a change back to complete growth medium at 6 h. Cells were used for in-culture drug metabolism assays 24 h after transfection. The transfection protocol for 96-well plates was the same as described for 6-well plates but scaled down proportionally (25-fold) to account for the decreased surface area of each well.

*Genotyping assay for CYP2E1*. Isolation of genomic DNA from mouse tails was performed as described previously (Sugamori *et al.*, 2003). The *Cyp2e1(−/−)* genotyping protocol was adapted from that described previously (Lee *et al.*, 1996). The wild-type allele was identified by the presence of a 125-bp PCR product using the primers 5′-AGT GTT CAC ACT GCA CCT GG-3′ (sense) and 5′-CCT GGA ACA CAG GAA TGT CC-3′ (antisense), each at a final concentration of 0.2 μM. The *Cyp2e1*(-) allele was identified by the presence of a 280-bp PCR product using the primers 5′-CTT GGG TGG AGA GGC TAT TC-3′ (sense) and 5′-TAC CGG TGG ATG TGG AAT G-3′ (antisense) each at a final concentration of 0.2 μM. Each PCR reaction also contained 0.2 mM dNTP, 2 mM $MgCl_2$, 1 × Taq buffer, 0.75 U Taq DNA polymerase, and 1 μl of template gDNA. The following PCR program was used for both wild-type and *Cyp2e1*(-) primers: 10 min at 94°C; 40 cycles of 15 s at 95°C, 20 s at 60°C, 20 s at 72°C; and 7 min at 72°C.

*Preparation of microsomes from mouse liver and cultured cells*. Animals were sacrificed by cervical dislocation. Livers were collected, snap frozen in liquid nitrogen, and stored at −80°C until processing. Livers were homogenized in 4 volumes of homogenization buffer (155 mM KCl, 10 mM potassium phosphate, pH 7.4) at 15 000 rpm for 20 s with a Polytron PT 1200E (Kinematica Inc, Bohemia, New York). Liver homogenates were centrifuged at 9000 × g for 20 min at 4°C, the supernatant was further centrifuged at 105 000 × g at 4°C for 1 h to pellet the microsomal fraction, the microsomal pellet was washed by resuspending in an equal volume of homogenization buffer and recentrifuging at 105 000 × g at 4°C for 1 h, and the final microsomal pellet was resuspended in storage buffer (10 mM Tris, 1 mM EDTA, 20% w/w glycerol, pH 7.4) to a final volume of 1 ml per gram of original liver weight, aliquoted, snap frozen in liquid nitrogen, and stored at −80°C. Protein concentrations in microsomal preparations were determined using the Bio-Rad Protein Assay.

In vitro *ABP N-hydroxylation assay*. Each *in vitro* ABP *N*-hydroxylation reaction contained 20 μl of 0.5 M potassium phosphate buffer pH 7.4, 10 μl of 2 mM ABP in 10% v/v acetonitrile, 25 μl of 20 mM $MgCl_2$, 5 μl of 10 mM NADP, 10 μl of 50 mM glucose-6-phosphate, 1 μl of 1 mg/ml glucose-6-phosphate dehydrogenase, and 29 μl of microsomal preparation (final concentration approximately 1 mg/ml) to a total volume of 100 μl. Reactions were incubated at 37°C for 10 min and terminated by the addition of 50 μl of ice-cold acetonitrile containing 0.3 mM ascorbic acid. After the removal of precipitated protein via centrifugation, 50 μl of the supernatant was injected onto a reverse phase C18 Beckman Ultrasphere 5-μm column (15 cm × 4.6 mm i.d.; Beckman Coulter, Fullerton, California) on a Shimadzu LC-2010 A system (Shimadzu Scientific Instruments Inc, Columbia, Maryland) at a flow rate of 2 ml/min. The HPLC mobile phase contained 25% w/w acetonitrile and 75% w/w of 20 mM sodium perchlorate buffer at pH 2.5. UV absorbance was measured at 280 nm and 35°C. Under these conditions, ABP and HOABP had retention times of 3.0 and 6.6 min, respectively. For the 1-aminobenzotriazole (ABT) inhibition experiment, reaction mixtures (minus ABP) were pre-incubated with ABT dissolved in EtOH (final concentration = 0.2% v/v) or with vehicle alone for 30 min at 37°C prior to reaction initiation with the addition of ABP.

In vitro *and in culture pNP hydroxylation assays*. Each *in vitro* *p*-nitrophenol (pNP) hydroxylation reaction contained 20 μl of 0.5 M potassium phosphate buffer pH 7.4, 10 μl of 2 mM pNP dissolved in $H_2O$, 25 μl of 20 mM $MgCl_2$, 5 μl of 10 mM NADP, 10 μl of 50 mM glucose-6-phosphate, 1 μl of 1 mg/ml glucose-6-phosphate dehydrogenase, and 29 μl of microsomal preparation (final concentration approximately 1 mg/ml) to a total volume of 100 μl. Reactions were incubated at 37°C for 30 min and terminated by the addition of 5 μl of 60% w/v $HClO_4$. After the removal of precipitated protein via centrifugation, 50 μl of the supernatant was injected onto the column described earlier and eluted at a flow rate of 1 ml/min. The HPLC mobile phase contained 25% w/w acetonitrile and 75% w/w of 0.1% w/w acetic acid. UV absorbance was measured at 345 nm and 35°C. Using these HPLC conditions, pNP and 4-nitrocatechol have retention times of 6.5 and 4.0 min, respectively. For the *in culture* pNP hydroxylation assay, pNP was added to cell culture medium to a final concentration of 200 μM and incubated with cells for 2 h. Following incubation, 100 μl of medium was withdrawn, mixed with 5 μl of 60% w/v $HClO_4$, centrifuged to remove precipitated protein, and 50 μl of the supernatant was analyzed by HPLC using the same conditions as described earlier for the *in vitro* assay.

*In culture phenacetin O-deethylation assay*. For the *in culture* phenacetin *O*-deethylation assay, phenacetin was added to cell culture medium to a final concentration of 200 μM and incubated with cells for 2 h. Following incubation, 100 μl of medium was withdrawn, mixed with 5 μl of 60% w/v $HClO_4$, centrifuged to remove protein precipitates, and 50 μl of the supernatant was quantified by HPLC using a flow rate of 1 ml/min and a mobile phase consisting of 10% w/w methanol and 90% w/w of 0.1% acetic acid. UV absorbance was measured at 245 nm and 35°C. Using these HPLC conditions, phenacetin and acetaminophen have retention times of 30 and 5 min, respectively.

*Quantification of γH2AX and NRF2 by immunoblotting*. γH2AX represents histone variant H2AX phosphorylated on serine 139. This phosphorylation event is triggered by DNA strand breaks, which represent one form of oxidative DNA damage, and is a rapid, initial event in DNA damage signaling. For the detection of levels of γH2AX and histone 3 (H3, loading control) in cultured cells, cells grown on six-well plates were washed twice with PBS and collected via scraping into 500 μl of sonication buffer (150 mM NaCl, 150 mM Tris–HCl, pH 7.4, 1 × protease inhibitors, and 1 × phosphatase inhibitors). Samples were kept on ice at all

times. Cells were lysed via sonication using a probe sonicator (ThermoFisher Scientific Inc) at 25% amplitude with $4 \times 5$ s bursts on ice. Protein concentrations in cell lysates were determined using the Bio-Rad Protein Assay. Samples were mixed with SDS–PAGE loading buffer, boiled at 95°C for 10 min, and loaded onto two 12.5% SDS–PAGE gels (20 μg protein per lane for the γH2AX and NRF2 gels, and 5 μg protein for the H3 gels). Both gels were electrophoresed simultaneously, transferred onto nitrocellulose membranes, blocked with 4% w/v powdered milk in TNT buffer (10 mM Tris–HCl, 150 mM NaCl, 0.05% v/v Tween 20, pH 8.0) for 2 h at room temperature and incubated with primary antibodies (3:5000 dilution for γH2AX and 1:500 000 dilution for H3) overnight at 4°C. Blots were then washed for $3 \times 5$ min with TNT buffer, incubated with secondary antibodies (anti-mouse for γH2AX in TNT buffer and anti-rabbit for H3 in blocking solution, both at 1:10 000 dilution), washed for $3 \times 10$ min, incubated for 2 min with ECL prime, exposed to X-ray films, and developed films were scanned and quantified by densitometry using Image J software (NIH). The average band intensity of vehicle-treated samples was arbitrarily assigned a value of 1, and all band intensities were normalized to this average intensity.

For the detection of γH2AX and H3 levels in liver tissue, livers were perfused with PBS, collected, snap frozen in liquid nitrogen, and stored at −80°C until processing. In total, 50 mg of liver was homogenized in 2.5 ml of homogenization buffer (5 mM $MgCl_2$, 50 mM Tris–HCl pH 7.6, 50 mM NaCl, 1 mM EDTA, 5% v/v glycerol, 0.1% w/w Triton X-100, and 0.1% β-mercaptoethanol). Contents were kept on ice at all times. The liver homogenate was centrifuged at $1100 \times g$ for 10 min, pelleted nuclei were resuspended in 500 μl of sonication buffer, and all subsequent steps were as described earlier for cell culture lysates, with the addition of a brief centrifugation at $1000 \times g$ for 2 min at 4°C after sonication to remove tissue debris. For NRF2, a 10% SDS–PAGE gel, a 1-h transfer period, and a 1:10 000 dilution of the antiserum were used.

*DCF assay*. Hepa1c1c7 cells were seeded at $3 \times 10^4$ cells per well into a 96-well plate and grown overnight. The next day, cells were incubated with 50 μM of freshly prepared dichlorofluorescein (DCF) dye in complete cell culture medium for 1 h, washed twice with 200 μl MEM (minus phenol red), treated with drugs of interest in 100 μl MEM (minus phenol red), and measured immediately on a fluorescence kinetic plate reader (BioTek Instruments Inc, Winooski, Vermont; 37°C, excitation = 485 nm, emission = 528 nm, 1 read/min for 30 min). Slopes of kinetic curves (rates of reactive oxygen species production) were recorded as the DCF signal. For transfected cells, cells were seeded at $2 \times 10^4$ cells per well onto a 96-well plate, grown overnight, transfected with the gene of interest on the second day, and tested using the DCF assay on the third day.

*RNA extraction and cDNA synthesis*. To extract RNA from liver, 10 mg of tissue was homogenized in 1 ml of TRIzol with a Polytron PT 1200E (Kinematica Inc) at 15 000 rpm for 20 s on ice. Subsequent RNA extraction steps were carried out following manufacturer's instructions. The quality and concentration of RNA samples were determined using a NanoDrop device (ThermoFisher Scientific Inc). The integrity of RNA was verified by the presence of intact 28S and 18S rRNA bands on an agarose gel. RNA samples were stored at −80°C.

Prior to reverse transcription, RNA was first treated with DNase I to remove potential DNA contamination. This was performed by incubating RNA with DNase I in the appropriate buffer for 30 min at 37°C. The DNase I reaction was terminated with the addition of EDTA followed by incubation for 10 min at 65°C. Reverse transcription was carried out using 1 μg of DNase I treated RNA in the presence of 0.5 mM dNTPs, $1 \times$ random hexamer primers, 0.01 M DTT, RiboLock RNase inhibitor, and M-MLV reverse transcriptase. The PCR program for reverse transcription was as follows: 25°C for 10 min, 37°C for 50 min, and 70°C for 15 min. Final cDNA products were stored at −20°C.

*Quantitative PCR analysis of NRF2 target gene expression*. qPCR was conducted using SYBR Green dye-based PCR and Applied Biosystems 7500 Fast Real-Time PCR System (Life Technologies Inc). The *Gapdh* gene was used as the endogenous control. Each qPCR reaction contained cDNA template, 0.4 μl each of forward and reverse primers (final concentrations indicated in Supplementary Table 1), 7.5 μl of SYBR Green, and made to a final volume of 15 μl with $dH_2O$. Cycling conditions for qPCR were as follows: 50°C for 2 min; 95°C for 10 min; 40 cycles of 95°C for 15 s followed by 60°C for 1 min.

qPCR primers were designed using the Primer-BLAST program provided by the National Center for Biotechnology Information website (National Library of Medicine, Bethesda, Maryland; www.ncbi.nlm.nih.gov). Primers were tested for annealing efficiency against the endogenous *Gapdh* control to ensure similar efficiencies. Primer annealing efficiency graphs were generated by measuring $C_t$ values over a range of cDNA concentrations for both the gene of interest and *Gapdh*, and plotting differences in $C_t$ values between these two genes on the y-axis against the log of [cDNA] on the x-axis. Primers for the gene of interest were considered to have similar annealing efficiencies as *Gapdh* primers when the primer annealing efficiency graph had a slope between −0.1 and 0.1. Only primers with similar annealing efficiencies as *Gapdh* were used for further experiments. Data analyses were carried out using the comparative $C_t$ method for relative quantification.

*Statistical analyses*. For competitive inhibition studies using ABP and pNP, non-linear regression analyses were carried out by modeling the inhibition data using GraphPad software (La Jolla, California) assuming single-site competitive inhibition.

## RESULTS

### *CYP2E1 is a Major ABP N-Hydroxylating Enzyme in Developing Mouse Liver Microsomes*

The *N*-hydroxylation of ABP appears to be involved in all of its known deleterious effects, including the generation of ABP-DNA adducts and oxidative stress, yet *in vivo* studies contradict the previously assumed role of CYP1A2 in carrying out this reaction (Kimura *et al.*, 1999). We therefore sought to identify additional major ABP *N*-hydroxylation enzymes present in mouse liver at the developmental stage corresponding to ABP exposure in the neonatal tumor bioassay. Specifically, we used liver microsomes isolated from postnatal day 15 mice, representing the age at which the second of two ABP exposures occurs in the bioassay protocol. We first tested ABP *N*-hydroxylation activity at a substrate concentration of 200 μM, a comparable concentration to that detected in mouse serum following exposure to ABP in a previous pharmacokinetic study (Sugamori *et al.*, 2006). Under these conditions, ABP *N*-hydroxylation activity was 34% lower in male *Cyp1a2(−/−)* mouse liver microsomes than in wild-type microsomes ($P < .05$), but not in the corresponding microsomes from female mice (Fig. 1A, two-way ANOVA followed by Bonferroni post-tests). These results suggest the presence of an

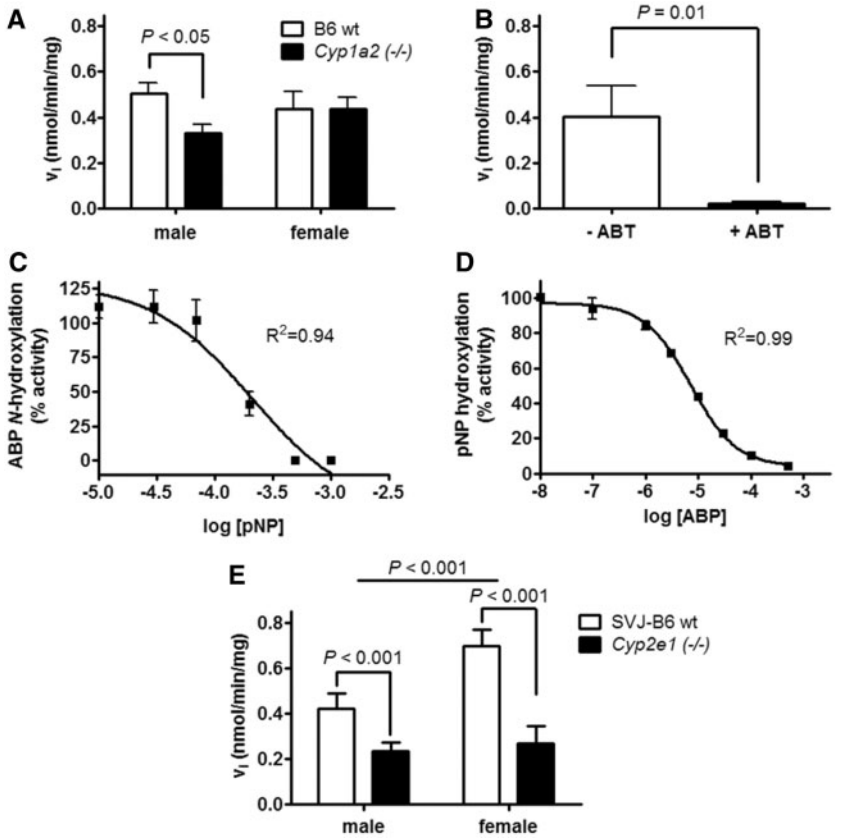


**FIG. 1.** Effects of pharmacological and genetic manipulations on ABP *N*-hydroxylation activity in mouse liver microsomes. A, ABP *N*-hydroxylation activity was measured in liver microsomes from postnatal day 15 wild-type and *Cyp1a2*(−/−) C57BL/6 mice ($N = 4$ per group). *P*-values were generated using two-way ANOVA followed by Bonferroni post hoc analyses. B, ABP *N*-hydroxylation activity was measured in liver microsomes from day 15 *Cyp1a2*(−/−) C57BL/6 mice in the presence or absence of 1 mM ABT ($N = 4$). *P*-value was generated using Student's *t* test. C, ABP *N*-hydroxylation activity was measured in liver microsomes from male postnatal day 15 *Cyp1a2*(−/−) C57BL/6 mice in the presence of varying concentrations of pNP ($N = 3$). D, pNP hydroxylation activity was measured in liver microsomes from male postnatal day 15 *Cyp1a2*(−/−) C57BL/6 mice in the presence of varying concentrations of ABP ($N = 3$). $R^2$ values were calculated by fitting curves to a one-site competition model. E, ABP *N*-hydroxylation activity was measured in liver microsomes from day 15 *Cyp2e1*(+/+) and *Cyp2e1*(−/−) SVJ-B6 mixed-strain mice ($N = 5$). *P*-values were generated using two-way ANOVA followed by Bonferroni post hoc analyses.

alternative ABP *N*-hydroxylating enzyme that is not CYP1A2, and which is responsible for the majority of ABP *N*-hydroxylation activity, especially in females, at this developmental stage.

To determine whether the alternative ABP *N*-hydroxylation enzyme represents a cytochrome P450, we tested the effect of the general cytochrome P450 inhibitor ABT on ABP *N*-hydroxylation by liver microsomes from postnatal day 15 *Cyp1a2*(−/−) mice. ABT inhibited the ABP *N*-hydroxylation activity by about 95% (Fig. 1B, $P = .01$ by Student's *t* test). In subsequent reaction phenotyping studies using *Cyp1a2*(−/−) microsomes we observed an unexpected solvent effect such that the commonly used laboratory solvents DMSO (Supplementary Fig. 1), methanol, and acetone (not shown) all inhibited the ABP *N*-hydroxylation reaction, whereas acetonitrile did not (Supplementary Fig. 1). Because this solvent inhibition profile matches that previously described for CYP2E1 (Hickman *et al.*, 1998), we tested the CYP2E1-selective substrate pNP as a potential inhibitor of ABP *N*-hydroxylation activity. pNP concentration-dependently inhibited ABP *N*-hydroxylation activity, with non-linear regression based on single-site competitive inhibition giving an $R^2$ value of 0.94 (Fig. 1C). ABP also concentration-dependently inhibited pNP hydroxylation, with an $R^2$ value of 0.99 (Fig. 1D). Finally, further evidence supporting a role for CYP2E1 in the *N*-hydroxylation of ABP was generated using *Cyp2e1*(−/−) mice. ABP *N*-hydroxylation activity in microsomes from *Cyp2e1*(−/−) mice was significantly lower in both males (44%) and females (61%) than in their corresponding wild-type controls ($P < .001$, Fig. 1E). It should be noted that *Cyp1a2*(−/−) and *Cyp2e1*(−/−) studies were carried out using mice of different genetic backgrounds, which may in turn lead to the apparent difference in ABP *N*-hydroxylation activity between their corresponding wild-type mice (Löfgren *et al.*, 2004).

### *HOABP but Not ABP Induces Oxidative Stress in Hepa1c1c7 Cells*

We determined whether ABP or HOABP can produce oxidative stress in a cell culture setting using the DCF assay as a measure of reactive oxygen species production. The HOABP metabolite (10 and 20 μM) induced significant increases in DCF signal in Hepa1c1c7 cells compared with vehicle-treated controls ($P < .001$, two-way ANOVA followed by Bonferroni post-tests), whereas the parent compound ABP did not (Fig. 2A, $P > .05$). The signal produced by HOABP was also prevented by the antioxidant *N*-acetylcysteine (NAC). We then used the immunoblot-based detection of γH2AX as a marker of oxidative DNA damage. ABP treatment failed to induce γH2AX in Hepa1c1c7 cells under a variety of different conditions (Fig. 2B–D). On the other hand, 10 μM ($P < .05$) and 20 μM ($P < .001$) HOABP significantly induced γH2AX (one-way ANOVA followed by Bonferroni post-tests, Fig. 2E). Again, co-treatment with NAC completely blocked the oxidative stress produced by HOABP (Fig. 2F).

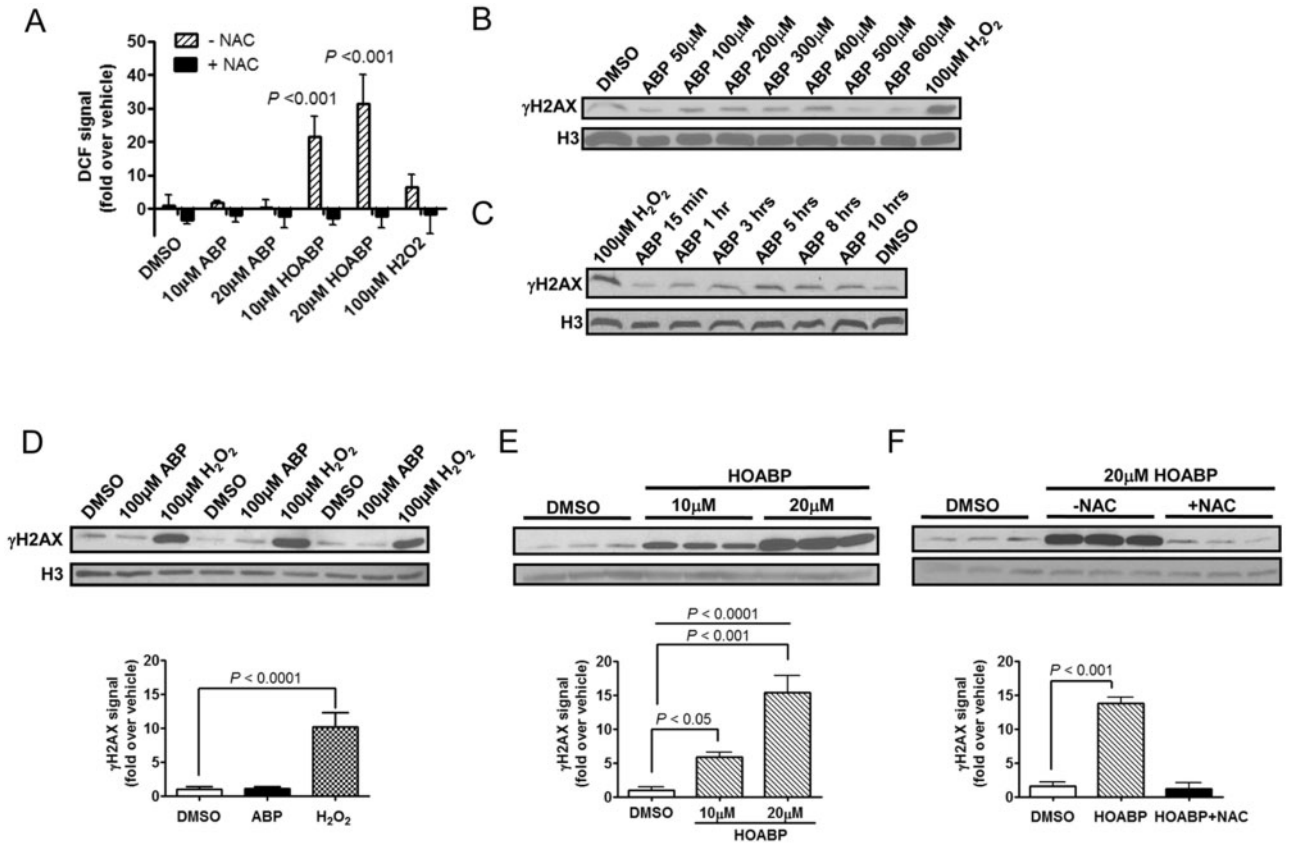


**FIG. 2.** Cellular oxidative stress responses to ABP and HOABP. A, Fluorometric quantification of DCF signal in Hepa1c1c7 cells treated with DMSO vehicle (0.1% v/v), ABP (10 and 20 μM), HOABP (10 and 20 μM), or 100 μM $H_2O_2$. Mean ± SD was calculated based on four replicates from a single experiment. *P*-values were generated by comparing to vehicle-treated controls using two-way ANOVA followed by Bonferroni post hoc analyses. B, Immunoblot from Hepa1c1c7 cells treated with DMSO vehicle (0.01% v/v), 50–600 μM of ABP, or 100 μM $H_2O_2$ for 4 h. C, Immunoblot from Hepa1c1c7 cells treated with DMSO vehicle (0.01% v/v) for 10 h, 100 μM of ABP for 0.25–10 h, or 100 μM $H_2O_2$ for 4 h. D, Immunoblot from Hepa1c1c7 cells treated with DMSO vehicle (0.01% v/v), 100 μM of ABP, or 100 μM $H_2O_2$ for 4 h and quantified using densitometry. E, Immunoblot from Hepa1c1c7 cells treated with DMSO vehicle (0.01% v/v), 10 or 20 μM of HOABP for 4 h and quantified using densitometry. F, Immunoblot from Hepa1c1c7 cells treated with DMSO vehicle (0.1% v/v), 20 μM of HOABP, or 20 μM of HOABP + 1 mM NAC for 4 h and quantified using densitometry. For all immunoblots, cell lysates were separated on a 12.5% SDS–PAGE gel, reacted with anti-γH2AX or H3 (loading control) antibodies, quantified using densitometry and analyzed using Image J software (NIH). Mean ± SD was calculated based on three replicates from a single experiment, and *P*-values were calculated using one-way ANOVA followed by Bonferroni post hoc analyses. All results shown were replicated in a separate experiment (data not shown).

### *N-Hydroxylation of ABP by CYP2E1 but Not CYP1A2 Produces Oxidative Stress in Hepa1c1c7 Cells*

Like most hepatoma cell lines, the expression of Phase I drug metabolism enzymes is severely compromised in Hepa1c1c7 cells, such that no CYP1A2 or CYP2E1 transcript expression or enzyme activity can be detected in untransfected cells (Supplementary Fig. 2). Using transient transfection, CYP1A2 and CYP2E1 were individually expressed in Hepa1c1c7 cells (Supplementary Fig. 2). ABP produced significant increases in both oxidative DNA damage ($P < .05$ by Student's *t* test, Fig. 3A) and reactive oxygen species ($P < .01$ by one-way ANOVA, Fig. 3B) compared with vehicle-treated controls in *Cyp2e1*-transfected Hepa1c1c7 cells. However, ABP failed to produce either oxidative DNA damage or reactive oxygen species in *Cyp1a2*- (Fig. 3C and 3D) or *Nat3*- (Fig. 3E and 3F) transfected cells ($P > .05$). NAT3 was used as a negative control as it possesses no oxidative enzyme activity (Sugamori *et al.*, 2007). To determine whether ABP-induced oxidative stress is related to CYP2E1 enzyme activity, we tested the effects of CYP2E1-selective alternative substrates on ABP-induced reactive oxygen species using the DCF assay. ABP-induced reactive oxygen species production in *Cyp2e1*-transfected Hepa1c1c7 cells was blocked by the CYP2E1 substrates pNP ($P < .001$) and chlorzoxazone (CLX, $P < .001$) as identified by one-way ANOVA followed by Bonferroni post-tests (Fig. 3G). Furthermore, co-treatment of ABP with the antioxidant NAC also blocked ABP-induced reactive oxygen species in *Cyp2e1*-transfected Hepa1c1c7 cells ($P < .001$, Fig. 3G).

Both human and rat CYP2E1 have recently been shown to be localized to mitochondria in addition to the endoplasmic reticulum (Bansal *et al.*, 2010, 2013). To examine the potential involvement of mitochondrial CYP2E1 in ABP-induced oxidative stress, we tested the effect of ABP on Hepa1c1c7 cells transiently transfected with different rat *Cyp2e1* variants that express CYP2E1 protein at similar total levels but target differentially between mitochondria and endoplasmic reticulum. These rat *Cyp2e1* variants rank from low to high expression in mitochondria in the following order: ER (20%) < WT (47%) < MT (58%) < MT++(85%), where the percentage in parentheses represents the proportion of total CYP2E1 protein expressed in the mitochondria of COS-7 cells (Bansal *et al.*, 2010). Treatment with 100 μM ABP significantly increased levels of reactive oxygen species in MT ($P < .05$) and MT++ ($P < .001$) rat *Cyp2e1* variant-transfected cells but not in ER or WT variant-transfected cells ($P > .05$) as revealed by two-way ANOVA followed by Bonferroni post-tests (Fig. 3H). Treatment with 500 μM ABP significantly increased levels of reactive oxygen species in WT ($P < .05$), MT ($P < .05$), and MT++

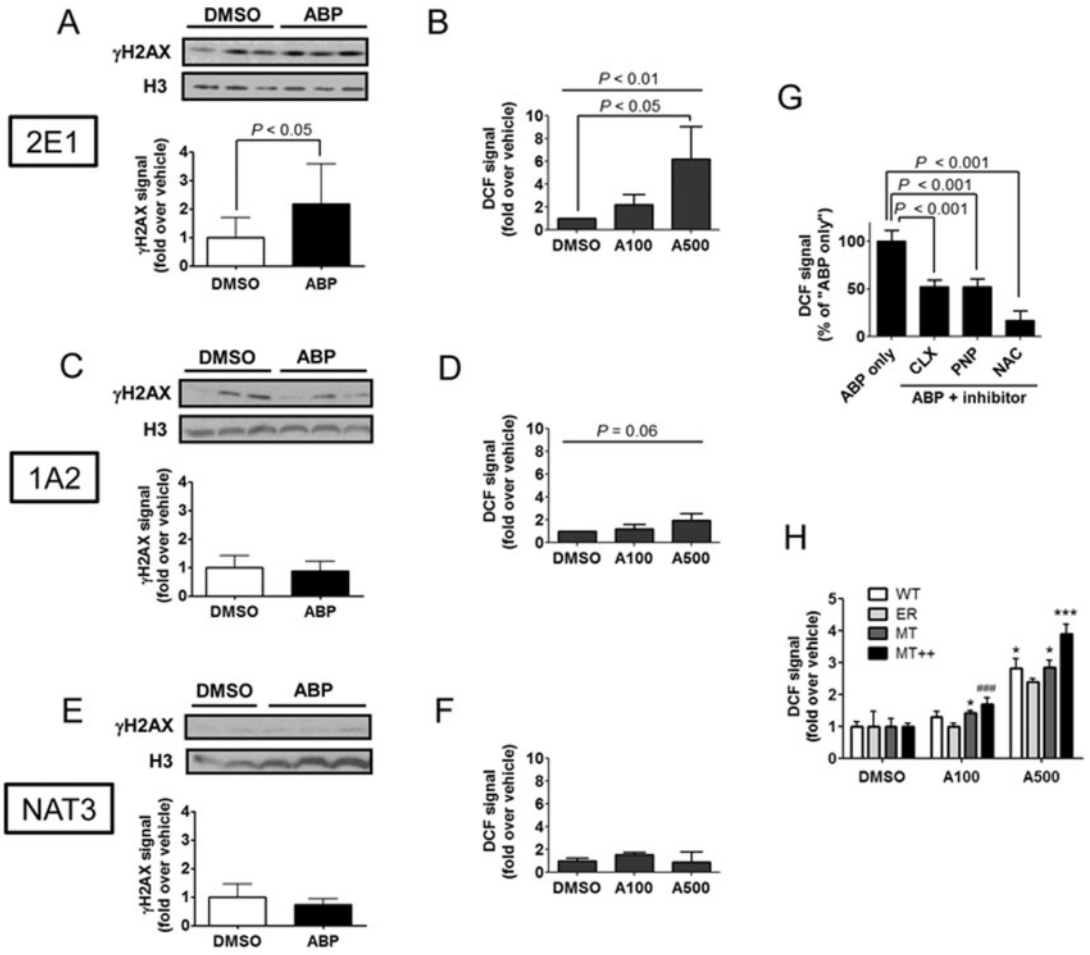


**FIG. 3.** Cellular oxidative stress response to ABP in the presence of ABP N-hydroxylation enzymes. Immunoblot from Hepa1c1c7 cells transiently transfected with *Cyp2e1* (A), *Cyp1a2* (C), or *Nat3* (E) treated with 0.1% v/v DMSO vehicle or 100 μM ABP. Cell lysates were separated on a 12.5% SDS–PAGE gel, subjected to immunoblot analysis with anti-γH2AX or H3 antibodies, quantified using densitometry, and analyzed by Image J software (NIH). A typical experiment is shown. Mean ± SD was calculated from three independent experiments. *P*-values were generated using Student's *t* test. Fluorometric quantification of DCF signal in Hepa1c1c7 cells transiently transfected with *Cyp2e1* (B), *Cyp1a2* (D), or *Nat3* (F), treated with 0.3% v/v DMSO vehicle, 100 μM ABP, or 500 μM ABP. Mean ± SD was calculated from three independent experiments. *P*-values were generated two-way ANOVA followed by Bonferroni post hoc analyses. G, Fluorometric quantification of DCF signal in Hepa1c1c7 cells transiently transfected with *Cyp2e1* and treated with 500 μM ABP alone or in combination with inhibitor (1 mM of CLX, pNP, or NAC). Mean ± SD was calculated from four replicates of a single experiment. *P*-values were generated using one-way ANOVA followed by Bonferroni post hoc analyses. Results were replicated in a separate experiment (data not shown). H, Fluorometric quantification of DCF signal in Hepa1c1c7 cells transiently transfected with different rat *Cyp2e1* variants and treated with 0.3% v/v DMSO vehicle, 100 μM ABP, or 500 μM ABP. Mean ± SD was calculated from four replicates of a single experiment. *P*-values were generated using two-way ANOVA followed by Bonferroni post hoc analyses. "****"$P < .001$ compared to all other variants. "###"$P < .001$ compared to the ER variant. "*"$P < .05$ compared to the ER variant. Results were replicated in a separate experiment (data not shown).

($P < .001$) but still not in ER ($P > .05$) rat *Cyp2e1* variant-transfected Hepa1c1c7 cells (Fig. 3H). Overall, the level of ABP-induced reactive oxygen species in Hepa1c1c7 cells was positively correlated with the extent of mitochondrial expression for each rat *Cyp2e1* variant, with MT++ > MT > WT ≥ ER.

### *A Tumor-Inducing Dose of ABP Generates Oxidative Stress in Male but Not Female Mouse Liver*

We determined whether ABP can produce oxidative stress *in vivo* following the postnatal ABP exposure protocol used in our neonatal tumor bioassay. We adapted our cell culture γH2AX detection method to measure γH2AX levels in male and female mouse liver 2, 7, and 24 h after an *in vivo* 1200 nmol dose of ABP. No change in oxidative DNA damage was observed at 2 h (data not shown). Compared to vehicle-treated controls, 1200 nmol ABP induced significantly higher oxidative DNA damage in male liver at both 7 ($P < .01$) and 24 h ($P < .05$) using Student's *t* test (Fig. 4A and 4C). In contrast, ABP failed to induce a significant increase in oxidative DNA damage in female liver at any time point tested (Fig. 4B and 4D; $P > .05$), despite similar basal levels of oxidative DNA damage in both sexes (Supplementary Fig. 4B). Finally, a postnatal day 8 dose of 400 nmol ABP (1/3 of the total tumor-inducing dose) failed to produce significantly increased oxidative DNA damage in either male or female mouse liver at 24 h (Supplementary Fig. 4A). No changes were observed in levels of reduced or oxidized glutathione or the ratio of reduced/oxidized glutathione after postnatal ABP exposure in either male or female mice (data not shown).

### *Deficiency in CYP2E1 but Not CYP1A2 Protects Males from ABP-Induced Oxidative Stress In vivo*

We tested the potential roles of ABP N-hydroxylation enzymes in the generation of oxidative DNA damage following a

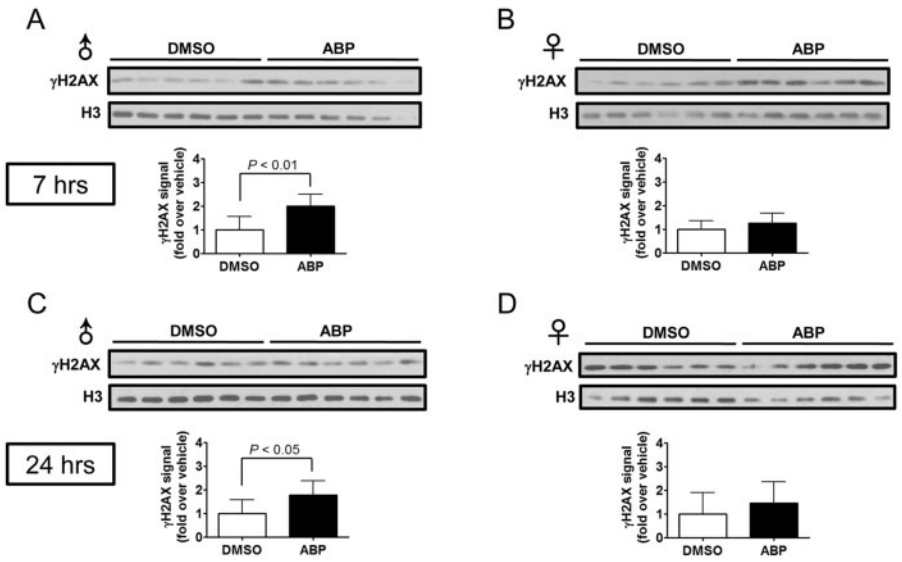


FIG. 4. *In vivo* levels of γH2AX after a tumor-inducing exposure to ABP. Immunoblot of nuclear γH2AX levels in male livers at 7 h (A) and 24 h (C) after the postnatal day 15 dose of ABP or DMSO vehicle (N = 6). Immunoblot showing nuclear γH2AX levels in neonatal female livers at 7 h (B) and 24 h (D) after the postnatal day 15 dose of ABP or DMSO vehicle (N = 6). Mean ± SD was normalized to mean of vehicle-treated samples, and *P*-values were generated using Student's *t* test. For immunoblots, liver nuclei homogenates were separated on a 12.5% SDS–PAGE gel, subjected to immunoblot analysis with anti-γH2AX or H3 antibodies, quantified using densitometry, and analyzed by Image J software (NIH).

tumor-inducing dose of ABP using *Cyp1a2(−/−)* and *Cyp2e1(−/−)* mice. Because *Cyp2e1(−/−)* mice are on a mixed-strain background, they were compared to their corresponding *Cyp2e1(+/+)* mixed-strain controls. At 7 h following the postnatal day 15 dose of ABP, *Cyp2e1(+/+)* males showed a significant increase in liver oxidative DNA damage (Student's *t* test, $P < .001$, Fig. 5A) that was not found in the corresponding females ($P > .05$) as measured using γH2AX (Fig. 5B), reproducing the sex difference observed in C57BL/6 mice shown in Figure 4. Interestingly, *Cyp2e1(−/−)* males were protected from liver oxidative DNA damage following ABP exposure (Student's *t* test, $P > .05$, Fig. 5C). On the other hand, *Cyp1a2(−/−)* males were not protected from liver oxidative DNA damage following a tumorigenic dose of ABP (Student's *t* test, $P < .01$, Fig. 5E). As was observed in wild-type mice (both C57BL/6 and *Cyp2e1(+/+)*), ABP did not induce γH2AX in female livers from either *Cyp2e1(−/−)* or *Cyp1a2(−/−)* mice (Student's *t* test, $P > .05$, Fig. 5D and 5F).

### *A Tumor-Inducing Dose of ABP Triggers a Stronger NRF2 Antioxidant Response in Female Than in Male Mouse Liver*

To further investigate the observed sex difference in ABP-induced oxidative stress *in vivo*, we measured the antioxidant response in mouse liver following a tumorigenic dose of ABP. We focused on the transcription factor NRF2, which represents a master regulator of the antioxidant response in mouse liver. At 24 h following the postnatal day 15 dose of ABP, the nuclear level of NRF2 was significantly increased in both male and female mouse liver (Fig. 6A and 6B). Compared to vehicle-treated controls, ABP-treated females showed greater NRF2 induction (Fig. 6B, approximately 6.3-fold, Student's *t* test, $P < .001$) than males (Fig. 6A, approximately 2.1-fold, Student's *t* test, $P < .01$), although the sexes had equal basal expression of NRF2 (Supplementary Fig. 4C). On the other hand, a postnatal day 8 dose of ABP (1/3 of the total tumor-inducing dose) produced no increase in nuclear NRF2 compared with vehicle-treated controls at 24 h (Supplementary Fig. 4A). To extend our NRF2 findings, we measured the effect of a tumorigenic dose of ABP on the expression of the antioxidant response genes *Ggt1*, *Nqo1*, and *Hmox1*, which are induced by oxidative stress and are at least in part regulated by NRF2 (Kensler *et al.*, 2007; Zhang *et al.*, 2006). ABP induced significant increases in the expression of all three genes, as revealed by Wilcoxon signed rank test (Fig. 6C–E). Interestingly, for two of the three genes, *Ggt1* and *Nqo1*, Bonferroni post-tests revealed significant induction by ABP only in females but not in males, demonstrating a female predominance in the induction of antioxidant genes by a tumor-inducing dose of ABP that is consistent with the greater elevation in the nuclear level of NRF2 in females.

## DISCUSSION

Previous studies from our laboratory and others using male and female mice deficient in key ABP bioactivation enzymes revealed a surprising lack of correlation between levels of ABP-DNA adducts or base-pair mutations and the liver tumorigenicity of ABP using the neonatal tumor bioassay exposure protocol (Kimura *et al.*, 1999; Sugamori *et al.*, 2012; Wang *et al.*, 2012). From these studies it was concluded that despite the well-established direct DNA-damaging effects of ABP metabolites and the previous implication of CYP1A2 in producing these metabolites, other as yet unidentified metabolic enzymes may play a key role in this process, and they may do so at least in part by mechanisms not arising from DNA adduct damage.

Given the presumed central importance of the ABP *N*-hydroxylation reaction in mediating the toxicity of ABP, we sought to identify additional ABP *N*-hydroxylating enzyme(s) in neonatal mice. A comparison of ABP *N*-hydroxylation activity between liver microsomes isolated from wild-type and *Cyp1a2(−/−)* mice revealed significant activity remaining in *Cyp1a2(−/−)* mice, confirming previous observations by Kimura *et al.* (1999). Characteristic inhibitory effects of various solvents and chemical probes on the remaining ABP *N*-hydroxylation activity in *Cyp1a2(−/−)* mouse liver microsomes allowed us to propose CYP2E1 as a potential ABP *N*-hydroxylating enzyme in

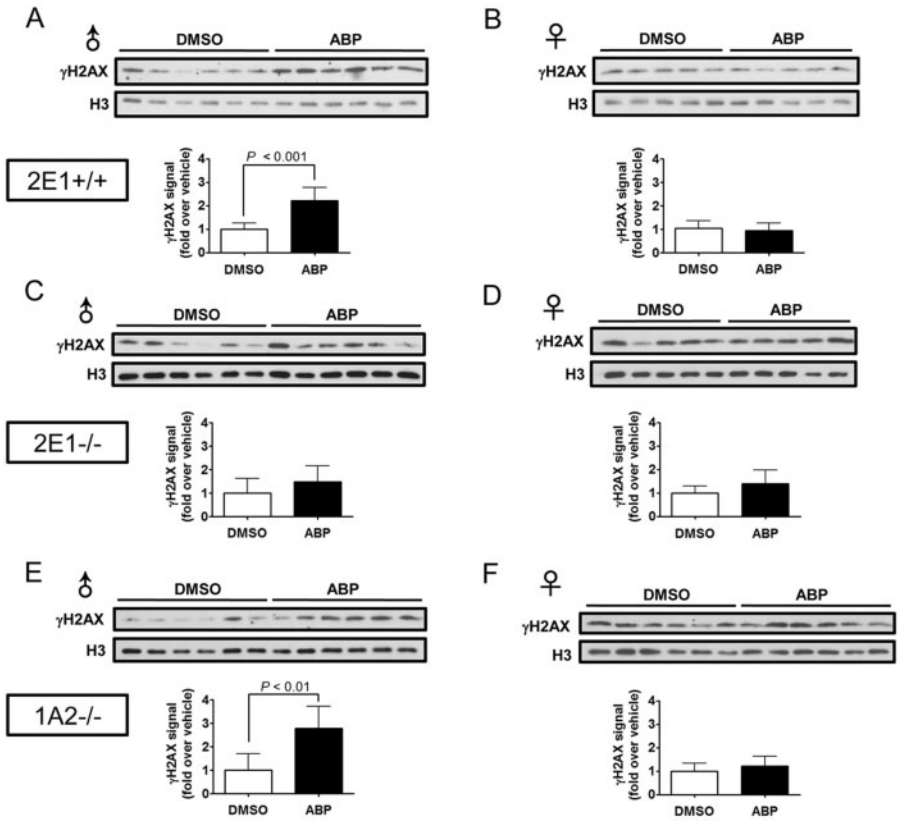


FIG. 5. Effects of ABP *N*-hydroxylation enzymes on the *in vivo* γH2AX response to a tumor-inducing dose of ABP. Immunoblot of nuclear γH2AX levels in male livers 7 h after the postnatal day 15 dose of ABP or DMSO vehicle in SVJ-B6 mixed-strain *Cyp2e1*(+/+) (A) or *Cyp2e1*(−/−) (C), or *Cyp1a2*(−/−) mice (E, N = 6). Immunoblot of γH2AX levels in female livers 7 h after the postnatal day 15 dose of ABP or DMSO vehicle in SVJ-B6 mixed-strain *Cyp2e1*(+/+) (B) or *Cyp2e1*(−/−) (D), or *Cyp1a2*(−/−) mice (F, N = 5–6). Mean ± SD for ABP-treated samples was normalized to mean of DMSO vehicle-treated samples, and *P*-values were generated using Student's *t* test. For immunoblots, liver nuclei homogenates were separated on a 12.5% SDS–PAGE gel, subjected to immunoblot analysis with anti-γH2AX or H3 antibodies, quantified using densitometry, and analyzed by Image J software (NIH).

developing mouse liver. Finally, a comparison of ABP *N*-hydroxylation rates between liver microsomes isolated from wild-type and *Cyp2e1*(−/−) mice revealed 44% and 61% reductions in activity in *Cyp2e1*(−/−) males and females, respectively, strongly supporting an important role for CYP2E1 in this reaction. To our knowledge, these results are the first to identify CYP2E1 as a major ABP *N*-hydroxylating enzyme in mouse liver, accounting for a significant proportion of the residual activity seen by us (Fig. 1A) and by others (Kimura *et al.*, 1999) in microsomes from *Cyp1a2*(−/−) mice. It will be of considerable interest to determine the extent to which CYP2E1 may also contribute to the *N*-oxidative bioactivation of other aromatic amine procarcinogens.

Together, our results indicate that CYP1A2 and CYP2E1 account for over one half of ABP *N*-hydroxylating activity found in neonatal mouse livers. However, it appears that significant activity remains that is likely attributed to yet other cytochrome(s) P450 that are also sensitive to inhibition by pNP, as this supposedly CYP2E1-selective substrate completely inhibited ABP *N*-hydroxylation activity in *Cyp1a2*(−/−) mice (Fig. 1C) while significant activity remained in *Cyp2e1*(−/−) mice (Fig. 1 E). The generation of *Cyp1a2/Cyp2e1* double knockout mice should aid in the conduct of experiments to identify these alternative ABP *N*-hydroxylation enzymes.

Given the close association of oxidative stress with human liver cancer (Hatting *et al.*, 2009; Hussain *et al.*, 2000) and evidence linking oxidative stress to ABP (Shertzer *et al.*, 2002; Tsuneoka *et al.*, 2003), we investigated oxidative stress as a novel driver of ABP-induced liver tumorigenesis in our neonatal bioassay. Using Hepa1c1c7 cells, we found that HOABP, but not the parent ABP, is a potent inducer of oxidative stress (Fig. 2). Our results are consistent with previous *in vitro* studies that have demonstrated strong redox properties for HOABP but not ABP (Makena and Chung, 2007; Murata *et al.*, 2001). However, our results are in contrast to results generated by another group, where ABP itself produced significant oxidative DNA damage in the human HepG2 hepatoma cell line (Wang *et al.*, 2006). This discrepancy may be attributed to the use of different cell culture conditions and/or cell lines with varying drug metabolizing potential. Specifically, the use of high concentrations of ABP for extended periods of time in the Wang *et al.* (2006) study may have led to significant cell death and associated DNA damage that is unrelated to the oxidative effects of ABP, a phenomenon that we have observed in our own experiments (S. Wang, unpublished observations).

To determine whether the *N*-hydroxylation of ABP leads to oxidative stress, we measured ABP-induced oxidative stress in Hepa1c1c7 cells transiently expressing CYP1A2 or CYP2E1. To our surprise, the *N*-hydroxylation of ABP by CYP2E1 but not CYP1A2 produced oxidative stress in Hepa1c1c7 cells (Fig. 3), even though we detected higher ABP *N*-hydroxylation activity in CYP1A2-expressing cells under our expression conditions (data not shown). A possible explanation for this apparent discrepancy lies with the recent discovery of mitochondria as a

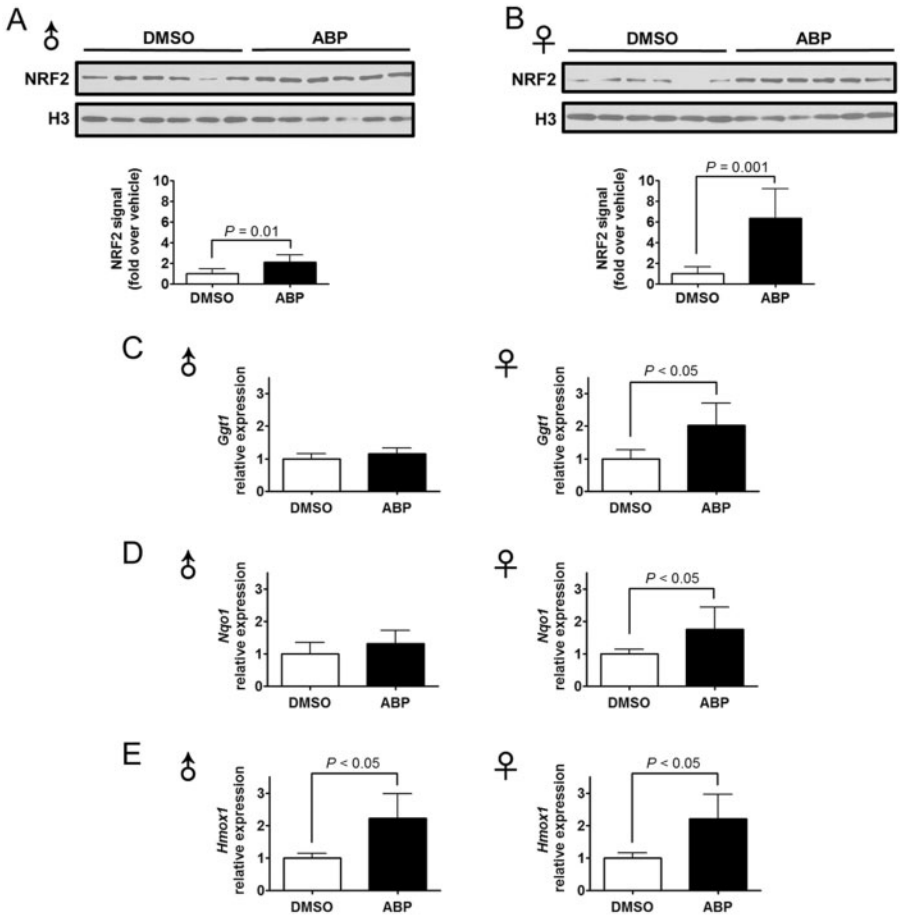


FIG. 6. *In vivo* NRF2 antioxidant response to a tumor-inducing exposure to ABP. Immunoblot showing nuclear levels of NRF2 in male (A) and female (B) livers 24 h after the postnatal day 15 dose of ABP or DMSO vehicle ($N = 6$). Mean ± SD for ABP-treated samples was normalized to the mean of DMSO vehicle-treated samples, and *P*-values were generated using Student's *t* test. qPCR was used to quantify levels of *Ggt1* (C), *Nqo1* (D), and *Hmox1* (E) gene expression in male and female livers 24 h after the postnatal day 15 dose of ABP or DMSO vehicle ($N = 7$ animals per group, each with three technical replicates). Means were normalized to the corresponding DMSO vehicle-treated group, and *P*-values were calculated based on delta $C_t$ values using the Wilcoxon signed rank test (two-tailed). For immunoblots, liver nuclei homogenates were separated on a 12.5% SDS–PAGE gel, subjected to immunoblot analysis with anti-NRF2 or H3 antibodies, quantified using densitometry, and analyzed by Image J software (NIH).

major localization site for CYP2E1, accounting for 10–40% of total CYP2E1 expression (Bansal *et al.*, 2010, 2013). The *N*-hydroxylation of ABP by mitochondrial CYP2E1 might result in HOABP production in the vicinity of the electron transport chain, leading to the increased reactive oxygen species production and oxidative stress observed in our cell culture studies. We tested this possibility by comparing the ability of ABP to produce oxidative stress in Hepa1c1c7 cells transfected with different rat CYP2E1 variants that target differentially between mitochondria and endoplasmic reticulum. We found that the level of reactive oxygen species produced by ABP was correlated with the extent of mitochondrial localization of rat CYP2E1, where the highest level of reactive oxygen species was found in cells transfected with the largely mitochondrial localized MT++ variant, despite these cells showing the lowest overall level of CYP2E1 transcript and activity (Supplementary Fig. 3). It is interesting to note that mitochondria may also be involved in the redox cycling properties of another often-studied carcinogenic aromatic amine derivative, 2-acetylaminofluorene (Klöhn *et al.*, 2003), raising the possibility that redox effects through interactions with mitochondria may represent a novel property of aromatic amines in general. Together, our cell transfection studies suggest that the *N*-hydroxylation of ABP by CYP2E1, perhaps in the vicinity of mitochondria, leads to oxidative stress in Hepa1c1c7 cells. Another possible explanation for observing ABP-induced oxidative stress in CYP2E1- but not CYP1A2-transfected cells is based on the unusually weak association between microsomal CYP2E1 and its electron donor, NADPH:P450 oxidoreductase, leading to the leakage of electrons that produce reactive oxygen species, at least *in vitro* (Gonzalez, 2005).

A tumorigenic exposure to ABP equivalent to that used in our tumor bioassay (Sugamori *et al.*, 2012) induced a significant increase in *in vivo* oxidative stress in neonatal mouse liver (Fig. 4). Interestingly, ABP produced a higher level of oxidative stress in males than in females, concordant with the male predominance in liver tumor incidence in the ABP neonatal bioassay. Similar sex differences have been observed in a previous study by Nebert *et al.*, where a 10 mg/kg dose of ABP dissolved in acetone applied to the dorsal skin of C57BL/6 adult mice led to significantly depleted hepatic thiols in male but not female wild-type liver by 2 h after ABP exposure (Tsuneoka *et al.*, 2003). We did not observe any depletion in hepatic total or reduced glutathione after postnatal ABP exposure, which may be due to differences in the age of the animals or the route of administration. To test for a possible effect of ABP *N*-hydroxylating

enzymes on ABP-induced oxidative stress *in vivo*, we compared ABP-induced oxidative DNA damage in livers from *Cyp2e1(−/−)* and *Cyp1a2(−/−)* mice and their corresponding wild-types. *Cyp2e1(−/−)* but not *Cyp1a2(−/−)* males were protected from ABP-induced oxidative DNA damage. These results are consistent with our cell culture findings, and together support the involvement of CYP2E1, but not CYP1A2, in the production of oxidative stress in developing mice following a tumorigenic dose of ABP. In all strains of mice tested, females were protected from ABP-induced oxidative DNA damage, suggesting sex differences that are conserved across different strains of mice.

As the NRF2 antioxidant response is a major modulator of liver oxidative stress, we investigated the effect of ABP on the NRF2 response in male and female neonatal mouse liver following the same exposure protocol as that used in our neonatal tumor bioassay. A tumorigenic dose of ABP significantly induced nuclear levels of NRF2 protein in both male and female neonatal liver compared with vehicle-treated controls. Interestingly, greater induction of NRF2 was observed in females than in males. We believe this is the first report of a sex difference in NRF2 activation following exposure to aromatic amines. In addition to nuclear levels of NRF2, ABP also induced the expression of the antioxidant genes *Ggt1*, *Nqo1*, and *Hmox1*, which are regulated at least in part by NRF2. Significant induction was seen in female but not male livers for *Ggt1* and *Nqo1*, whereas there was no sex difference in the induction of *Hmox1*. The lack of a sex difference in *Hmox1* induction by ABP may be due to the existence of additional transcription factors that regulate *Hmox1* expression in concert with NRF2, such as AP1 (Dalton *et al.*, 1999). In general, our results suggest that a stronger antioxidant response occurs in females than in males, as measured using NRF2 and NRF2-regulated antioxidant genes, which may protect females against liver oxidative stress induced by ABP. The magnitude of the gene expression changes we observed using ABP is comparable to other studies that have investigated NRF2-regulated genes in mouse liver following acute chemical exposure. For instance, a hepatotoxic 400 mg/kg i.p. dose of acetaminophen produced 2- and 3-fold increases in the expression of the *Nqo1* and *Hmox1* genes, respectively (Rohrer *et al.*, 2014).

Several mechanisms exist that may relay sex differences in ABP-induced acute oxidative stress to sex differences in ABP-induce liver tumorigenesis. For example in male mice, acute oxidative stress in the vicinity of the mitochondria may damage mitochondrial DNA, which in turn produces dysfunctional components of the electron transport chain leading to more oxidative stress. This vicious cycle may result in a state of chronic oxidative stress and associated cellular damage that promote liver tumorigenesis (Chatterjee *et al.*, 2006). Alternatively, acute oxidative stress and/or dysfunctional mitochondria in male mice may trigger a chronic inflammatory response through the activation of HMGB1, TLRs, NFκB, and/or inflammasomes that in turn promotes liver tumorigenesis (Lugrin *et al.*, 2014).

In summary, we have found that the bioactivation of ABP by CYP2E1 in developing mice leads to greater oxidative stress in males, whereas a stronger NRF2 antioxidant response may be protecting females from ABP-induced oxidative stress. These findings represent the first demonstration of sex differences in measures of ABP-induced toxicity that correlate with those in liver tumor incidence, and together they support oxidative stress as a significant driver of ABP tumorigenesis. In 2008, the International Agency for Research on Cancer estimated that liver cancer is the fifth most common cancer in men and the seventh in women (Ferlay *et al.*, 2010). Such high incidences of liver cancer strongly advocate for a better understanding of its underlying mechanisms, which may lead to novel prevention measures and drug targets. As ABP produces liver tumors in mice with a sex preference that parallels the 3- to 4-fold higher liver cancer incidence seen in men than in women, our results suggest that oxidative stress might also be one potential driver of the sex differences seen in human liver cancer.

## SUPPLEMENTARY DATA

Supplementary data are available online at http://toxsci.oxfordjournals.org/.

## FUNDING

An Operating Grant from the Institute of Gender and Health of the Canadian Institutes of Health Research (CIHR).

## ACKNOWLEDGMENTS

We would like to thank Shigeyuki Uno and Narayan Avadhani for the CYP1A2 and rat CYP2E1 expression plasmids, respectively. We would like to thank Daniel Nebert and Frank Gonzalez for *Cyp1a2(−/−)* and *Cyp2e1(−/−)* mice, respectively. We would like to thank Ed Schmidt for providing the NRF2 expression plasmid and antiserum.

## REFERENCES

Altekruse, S. F., McGlynn, K. A., and Reichman, M. E. (2009). Hepatocellular carcinoma incidence, mortality, and survival trends in the United States from 1975 to 2005. *J. Clin. Oncol.* **27,** 1485–1491.

Bansal, S., Anandatheerthavarada, H. K., Prabu, G. K., Milne, G. L., Martin, M. V., Guengerich, F. P., and Avadhani, N. G. (2013). Human cytochrome P450 2E1 mutations that alter mitochondrial targeting efficiency and susceptibility to ethanol-induced toxicity in cellular models. *J. Biol. Chem.* **288,** 12627–12644.

Bansal, S., Liu, C., Sepuri, N. B. V., Anandatheerthavarada, H. K., Selvaraj, V., Hoek, J., Milne, G. L., Guengerich, F. P., and Avadhani, N. G. (2010). Mitochondria-targeted cytochrome P450 2E1 induces oxidative damage and augments alcohol-mediated oxidative stress. *J. Biol. Chem.* **285,** 24609–24619.

Besaratinia, A., and Tommasi, S. (2013). Genotoxicity of tobacco smoke-derived aromatic amines and bladder cancer: Current state of knowledge and future research directions. *FASEB J.* **27,** 2090–2100.

Bosch, F. X., Ribes, J., Díaz, M., and Cléries, R. (2004). Primary liver cancer: Worldwide incidence and trends. *Gastroenterology* **127,** S5–S16.

Butler, M. A., Iwasaki, M., Guengerich, F. P., and Kadlubar, F. F. (1989). Human cytochrome P-450PA (P-450IA2), the phenacetin O-deethylase, is primarily responsible for the hepatic 3-demethylation of caffeine and N-oxidation of carcinogenic arylamines. *Proc. Natl. Acad. Sci. U.S.A.* **86,** 7696–7700.

Chatterjee, A., Mambo, E., and Sidransky, D. (2006). Mitochondrial DNA mutations in human cancer. *Oncogene* **25,** 4663–4674.

Chen, C. J., Yu, M. W., and Liaw, Y. F. (1997). Epidemiological characteristics and risk factors of hepatocellular carcinoma. *J. Gastroenterol. Hepatol.* **12,** S294–S308.

Chou, H. C., Lang, N. P., and Kadlubar, F. F. (1995). Metabolic activation of the N-hydroxy derivative of the carcinogen 4-aminobiphenyl by human tissue sulfotransferases. *Carcinogenesis* **16,** 413–417.

Dalton, T. P., Shertzer, H. G., and Puga, A. (1999). Regulation of gene expression by reactive oxygen. *Annu. Rev. Pharmacol. Toxicol.* **39,** 67–101.

Feng, Z., Hu, W., Rom, W. N., Beland, F. A., and Tang, M. (2002). N-hydroxy-4-aminobiphenyl-DNA binding in human p53 gene: Sequence preference and the effect of C5 cytosine methylation. *Biochemistry (N.Y.)* **41,** 6414–6421.

Ferlay, J., Shin, H., Bray, F., Forman, D., Mathers, C., and Parkin, D. M. (2010). Estimates of worldwide burden of cancer in 2008: GLOBOCAN 2008. *Int. J. Cancer* **127,** 2893–2917.

Gonzalez, F. J. (2005). Role of cytochromes P450 in chemical toxicity and oxidative stress: Studies with CYP2E1. *Mutat. Res.* **569,** 101–110.

Grimmer, G., Dettbarn, G., Seidel, A., and Jacob, J. (2000). Detection of carcinogenic aromatic amines in the urine of non-smokers. *Sci. Total Environ.* **247,** 81–90.

Hatting, M., Trautwein, C., and Cubero, F. (2009). TAL deficiency, all roads lead to oxidative stress?. *Hepatology* **50,** 979–981.

Hickman, D., Wang, J., Wang, Y., and Unadkat, J. D. (1998). Evaluation of the selectivity of in vitro probes and suitability of organic solvents for the measurement of human cytochrome P450 monooxygenase activities. *Drug Metab. Dispos.* **26,** 207–215.

Hussain, S. P., Raja, K., Amstad, P. A., Sawyer, M., Trudel, L. J., Wogan, G. N., Hofseth, L. J., Shields, P. G., Billiar, T. R., Trautwein, C., *et al.* (2000). Increased p53 mutation load in nontumorous human liver of wilson disease and hemochromatosis: Oxyradical overload diseases. *Proc. Natl. Acad. Sci. U.S.A.* **97,** 12770–12775.

Kensler, T. W., Wakabayashi, N., and Biswal, S. (2007). Cell survival responses to environmental stresses via the Keap1-Nrf2-ARE pathway. *Annu. Rev. Pharmacol. Toxicol.* **47,** 89–116.

Kim, C., Koike, K., Saito, I., Miyamura, T., and Jay, G. (1991). HBx gene of hepatitis B virus induces liver cancer in transgenic mice. *Nature* **351,** 317–320.

Kimura, S., Kawabe, M., Ward, J. M., Morishima, H., Kadlubar, F. F., Hammons, G. J., Fernandez-Salguero, P., and Gonzalez, F. J. (1999). CYP1A2 is not the primary enzyme responsible for 4-aminobiphenyl-induced hepatocarcinogenesis in mice. *Carcinogenesis* **20,** 1825–1830.

Klöhn, P., Soriano, M. E., Irwin, W., Penzo, D., Scorrano, L., Bitsch, A., Neumann, H., and Bernardi, P. (2003). Early resistance to cell death and to onset of the mitochondrial permeability transition during hepatocarcinogenesis with 2-acetylaminofluorene. *Proc. Natl. Acad. Sci. U.S.A.* **100,** 10014–10019.

Lee, S. S. T., Buters, J. T. M., Pineau, T., Fernandez-Salguero, P., and Gonzalez, F. J. (1996). Role of CYP2E1 in the hepatotoxicity of acetaminophen. *J. Biol. Chem.* **271,** 12063–12067.

Liang, H. C., Li, H., McKinnon, R. A., Duffy, J. J., Potter, S. S., Puga, A., and Nebert, D. W. (1996). Cyp1a2(-/-) null mutant mice develop normally but show deficient drug metabolism. *Proc. Natl. Acad. Sci. U.S.A* **93,** 1671–1676.

Löfgren, S., Hagbjörk, A. L., Ekman, S., Fransson-Steen, R., and Terelius, Y. (2004). Metabolism of human cytochrome P450 marker substrates in mouse: A strain and gender comparison. *Xenobiotica* **34,** 811–834.

Lugrin, J., Rosenblatt-Velin, N., Parapanov, R., and Liaudet, L. (2014). The role of oxidative stress during inflammatory processes. *Biol. Chem.* **395,** 203–230.

Makena, P. S., and Chung, K. (2007). Evidence that 4-aminobiphenyl, benzidine, and benzidine congeners produce genotoxicity through reactive oxygen species. *Environ. Mol. Mutagen.* **48,** 404–413.

McClain, R. M., Keller, D., Casciano, D., Fu, P., Macdonald, J., Popp, J., and Sagartz, J. (2001). Neonatal mouse model: Review of methods and results. *Toxicol. Pathol.* **29,** 128–137.

Minchin, R. F., Reeves, P. T., Teitel, C. H., McManus, M. E., Mojarrabi, B., Ilett, K. F., and Kadlubar, F. F. (1992). N- and O-acetylation of aromatic and heterocyclic amine carcinogens by human monomorphic and polymorphic acetyltransferases expressed in COS-1 cells. *Biochem. Biophys. Res. Commun.* **185,** 839–844.

Murata, M., Tamura, A., Tada, M., and Kawanishi, S. (2001). Mechanism of oxidative DNA damage induced by carcinogenic 4-aminobiphenyl. *Free Radic. Biol. Med.* **30,** 765–773.

National Toxicology Program. (2014). 13th Report on Carcinogens [Internet]. Available at: http://ntp.niehs.nih.gov/pubhealth/roc/roc13/index.html. Accessed November 15, 2014.

Naugler, W. E., Sakurai, T., Kim, S., Maeda, S., Kim, K., Elsharkawy, A. M., and Karin, M. (2007). Gender disparity in liver cancer due to sex differences in MyD88-dependent IL-6 production. *Science* **317,** 121–124.

Novak, M., Kahley, M. J., Eiger, E., Helmick, J. S., and Peters, H. E. (1993). Reactivity and selectivity of nitrenium ions derived from ester derivatives of carcinogenic N-(4-biphenylyl)hydroxylamine and the corresponding hydroxamic acid. *J. Am. Chem. Soc.* **115,** 9453–9460.

Orzechowski, A., Schrenk, D., Schut, H. A. J., and Bock, K. W. (1994). Consequences of 3-methylcholanthrene-type induction for the metabolism of 4-aminobiphenyl in isolated rat hepatocytes. *Carcinogenesis* **15,** 489–494.

Parsons, B. L., Beland, F. A., Von Tungeln, L. S., Delongchamp, R. R., Fu, P. P., and Heflich, R. H. (2005). Levels of 4-aminobiphenyl-induced somatic H-ras mutation in mouse liver DNA correlate with potential for liver tumor development. *Mol. Carcinog.* **42,** 193–201.

Rohrer, P. R., Rudraiah, S., Goedken, M. J., and Manautou, J. E. (2014). Is nuclear factor erythroid 2-related factor 2 responsible for sex differences in susceptibility to acetaminophen-induced hepatotoxicity in mice? *Drug Metab. Dispos.* **42,** 1663–1674.

Shertzer, H. G., Dalton, T. P., Talaska, G., and Nebert, D. W. (2002). Decrease in 4-aminobiphenyl-induced methemoglobinemia in Cyp1a2(-/-) knockout mice. *Toxicol. Appl. Pharmacol.* **181,** 32–37.

Sugamori, K. S., Brenneman, D., and Grant, D. M. (2006). In vivo and in vitro metabolism of arylamine procarcinogens in acetyltransferase-deficient mice. *Drug Metab. Dispos.* **34,** 1697–1702.

Sugamori, K. S., Brenneman, D., Sanchez, O., Doll, M. A., Hein, D. W., Pierce, W. M., Jr, and Grant, D. M. (2012). Reduced 4-aminobiphenyl-induced liver tumorigenicity but not DNA damage in arylamine N-acetyltransferase null mice. *Cancer Lett.* **318,** 206–213.

Sugamori, K. S., Brenneman, D., Wong, S., Gaedigk, A., Yu, V., Abramovici, H., Rozmahel, R., and Grant, D. M. (2007). Effect of arylamine acetyltransferase Nat3 gene knockout on N-acetylation in the mouse. *Drug Metab. Dispos.* **35,** 1064–1070.

Sugamori, K. S., Wong, S., Gaedigk, A., Yu, V., Abramovici, H., Rozmahel, R., and Grant, D. M. (2003). Generation and functional characterization of arylamine N-acetyltransferase

Nat1/Nat2 double knockout mice. *Mol. Pharmacol.* **64,** 170–179.

Tsuneoka, Y., Dalton, T. P., Miller, M. L., Clay, C. D., Shertzer, H. G., Talaska, G., Medvedovic, M., and Nebert, D. W. (2003). 4-Aminobiphenyl-induced liver and urinary bladder DNA adduct formation in Cyp1a2(-/-) and Cyp1a2(+/+) mice. *J. Natl. Cancer Inst.* **95,** 1227–1237.

Wang, S., Sugamori, K. S., Brenneman, D., Hsu, I., Calce, A., and Grant, D. M. (2012). Influence of arylamine N-acetyltransferase, sex, and age on 4-aminobiphenyl-induced in vivo mutant frequencies and spectra in mouse liver. *Environ. Mol. Mutagen.* **53,** 350–357.

Wang, S. C., Chung, J., Chen, C., and Chen, S. (2006). 2- and 4-aminobiphenyls induce oxidative DNA damage in human hepatoma (Hep G2) cells via different mechanisms. *Mutat. Res. Fundam. Mol. Mech. Mutagen.* **593,** 9–21.

Zhang, H., Liu, H., Dickinson, D. A., Liu, R., Postlethwait, E. M., Laperche, Y., and Forman, H. J. (2006). $\gamma$-Glutamyl transpeptidase is induced by 4-hydroxynonenal via EpRE/Nrf2 signaling in rat epithelial type II cells. *Free Radic. Biol. Med.* **40,** 1281–1292.